

Library

COPY 1

**NASA TECHNICAL
MEMORANDUM**



NASA TM X-1026

NASA TM X-1026

[Faint, illegible handwritten notes and stamps]

**PRELIMINARY EXPERIMENTAL OPERATION
OF HIGH-VOLTAGE ISOLATION DEVICE FOR
PROPELLANT SYSTEM OF AN ION ROCKET**

by Shigeo Nakanishi and Eugene V. Pawlik

Lewis Research Center

Cleveland, Ohio

**ADVANCE
COPY**

PRELIMINARY EXPERIMENTAL OPERATION OF HIGH-VOLTAGE
ISOLATION DEVICE FOR PROPELLANT SYSTEM
OF AN ION ROCKET

by Shigeo Nakanishi and Eugene V. Pawlik
Lewis Research Center
Cleveland, Ohio

NATIONAL AERONAUTICS AND SPACE ADMINISTRATION

TECHNICAL MEMORANDUM

PRELIMINARY EXPERIMENTAL OPERATION OF HIGH-VOLTAGE
ISOLATION DEVICE FOR PROPELLANT SYSTEM
OF AN ION ROCKET

by Shigeo Nakanishi and Eugene V. Pawlik

ABSTRACT

Preliminary experiments indicate that simple screens are a promising solution to the problem of electrical isolation of high-voltage electric thrusters from their propellant tank. A nonconducting propellant-feed tube with a conical-shaped screen across the tube has been operated with mercury-propellant electron-bombardment thrusters with voltages up to 6000 volts. Leakage currents are negligible, and it appears that waste heat from the thruster system will suffice to maintain tube temperatures above the condensation point.

E-2742

PRELIMINARY EXPERIMENTAL OPERATION OF HIGH-VOLTAGE
ISOLATION DEVICE FOR PROPELLANT SYSTEM
OF AN ION ROCKET

by Shigeo Nakanishi and Eugene V. Pawlik
Lewis Research Center

SUMMARY

Preliminary experiments indicate that simple screens are a promising solution to the problem of electrical isolation of high-voltage electric thrusters from their propellant tank. A nonconducting propellant-feed tube with a conical-shaped screen across the tube has been operated with mercury-propellant electron-bombardment thrusters with voltages up to 6000 volts. Leakage currents are negligible, and it appears that waste heat from the thruster system will suffice to maintain tube temperatures above the condensation point.

INTRODUCTION

A method of separating the high voltage of ion thrusters from the propellant storage tank is desirable for a variety of reasons. A device of this type would ease the electrical insulation and control problems of the feed system for a single module and would simplify overload protection circuitry when applied to an array of thrusters.

A simple passive device for accomplishing high-voltage isolation of the thruster from the propellant system is described herein. The results of its use with electron-bombardment ion thrusters are presented. To date, the investigation has been confined to single-module operation. These results, however, are considered to be of sufficient immediate interest to electric propulsion technology to justify an early dissemination of this preliminary data.

Ion thrusters employing 5- and 20-centimeter-diameter electron-bombardment ion sources were used in this study. A description of the electron-bombardment thruster and the associated electrical circuitry is given in references 1 and 2.

APPARATUS

Figure 1 shows the vacuum facility installation of a 5-centimeter-diameter thruster with the high-voltage isolation tube between the thruster and the propellant-vapor source. A schematic drawing of the apparatus

E-2742

used in these tests is shown in figure 2. The propellant-feed system consists of a steam-jacketed vaporizer with interchangeable orifices. The feed system is isolated from the thruster by a 5.1-centimeter-diameter by 30.5-centimeter-long glass tube, shown schematically in figure 2. In the present experiment, the glass tube was heated to about 100°C by a heating coil in order to prevent mercury condensation. For a flight version, waste heat from the thruster could probably be used for this purpose.

A fine-mesh conical-shaped screen (plasma containment grid) is located within the glass insulator and serves to prevent the plasma from electrically coupling the thruster to the feed system. A minimum distance L is maintained between the feed system and the plasma containment grid depending on thruster operating potential and flow rates. A conical shape of the containment grid was used to provide a large surface area, and hence a large total open flow area, for a screen of a given blockage. The plasma is restrained principally by the small dimensions of the openings in the screen that are less than the sheath thickness formed at the plasma boundaries. Two screens of different mesh size are shown in figure 3.

The power supplies required to operate the thruster and the variables that were metered are shown in figure 4. Leakage current from the vaporizer to ground J_L was also metered. The containment grid potential was measured with respect to the anode or net accelerating potential by means of a calibrated high-impedance meter isolated above ground. Three of the thruster power supplies may be considered internal in that they supply power at voltages that are relative to the anode of the thruster. These are the supplies for energizing the magnetic-field winding, heating the cathode, and establishing the discharge voltage. The two high-voltage supplies provide the potential difference between the electrodes that focus and accelerate the exhaust beam.

The ion thrusters were mounted in a 36-inch-diameter bell jar that was exhausted through a 36-inch valve into a 5-foot-diameter by 16-foot-long vacuum tank (fig. 5).

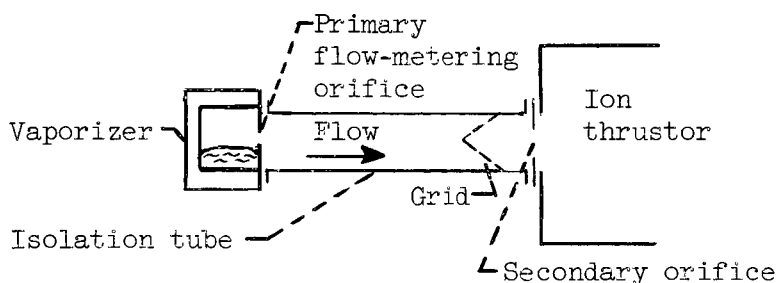
PROCEDURE

Thruster startup and operating procedure was no different from the conventional procedure described in reference 1, with the exception of a tube preheating period to avoid condensation of the propellant. When the entire system reached stable operating temperatures, several check points were taken to verify that the thruster was operating normally.

The voltage at which electrical breakdown occurred through the tube, that is, the critical voltage, was determined by increasing the net accelerating, or anode, voltage in steps of 500 or 1000 volts. The decelerating voltage was held at -1500 volts, which was found adequate to prevent electron backstreaming at all anode voltages applied. Each voltage level was maintained long enough to record all the meter readings and to assure

essentially equilibrium operation without a tube discharge. Lower breakdown voltages might have been obtained with operation for periods of hours at each voltage level, but the difference would be expected to be small.

Various pressure levels of the mercury vapor within the tube were established by varying the neutral propellant flow rate. An alternate method used in raising the tube pressure is shown in the accompanying sketch. A secondary orifice was installed in the propellant flow passage



between the grid and the thruster. Different sizes of the primary flow-metering orifice in the vaporizer were used in conjunction with the secondary orifice. A wide range of tube pressure was thus obtained without imposing an excessive propellant flow rate upon the thruster.

RESULTS AND DISCUSSION

General Operating Characteristics

The device reported herein resembles a class of low-pressure glow discharge tubes that have been extensively reported in the literature (e.g., ref. 3). The presence of the plasma containment grid, however, affects the operational behavior of the tube markedly. A tube as long as 90 centimeters was installed without the containment grid and net accelerating voltage was applied both with and without the ionization chamber in operation. A voltage of 2500 volts could be maintained indefinitely with no visible discharge when the ionization chamber was not operating. With the ionization chamber in operation, however, the same accelerating voltage could be held for only a short time interval before onset of a mercury-vapor discharge extending the entire length of the tube. In some instances, the tube discharge would occur with only the ionization chamber operating at the normal value of 50 volts and with no accelerating voltage applied.

With the grid installed, normal thruster operation could be maintained indefinitely at any net accelerating voltage lower than the critical voltage. A visible blue glow of uniform intensity normally extends from the ionization chamber up to the containment grid but not beyond it. With the grid at

floating potential, the leakage current to the grounded vaporizer is of the order of a few microamperes. At increasingly higher accelerating voltages, the grid potential becomes erratic. Oscillograms indicate the presence of voltage spikes with a steep front and a noticeable decay time of the order of 2 milliseconds. The leakage current to ground is not greatly increased until the onset of tube discharge, at which time the current rises suddenly to the value limited by the surge resistor in the high-voltage circuit. The discharge can be extinguished only by removing both the net accelerating voltage and the decelerating voltage normally held at 1500 volts negative with respect to ground.

The use of surge resistors greatly reduces the number of high-voltage breakdowns commonly encountered with the conventional thruster configuration in which the vaporizer is integral with the thruster body. As described in reference 4, these breakdowns may be interelectrode arcs or low-voltage arcs within the ionization chamber. They are significant because their occurrence generally triggers a discharge in the isolation tube. Possibly the highly energetic electrons or ions released from an arc within the thruster escape the containment grid causing ionization to occur within the tube. Ions thus formed are in an accelerating potential gradient such that positive ion bombardment of the grounded vaporizer causes sufficient secondary electron emission to establish a discharge. In some instances, however, an interelectrode arc may be of sufficient duration and intensity to trip the high-voltage power-supply breaker but have no apparent effect on the isolation tube.

A detailed study of the transient behavior and the contributing mechanisms underlying the operational characteristics of the present isolation device is beyond the scope of this report. Preliminary results covering the steady-state operational regime and the effects of what are considered to be pertinent variables are presented in the subsequent sections.

Propellant Flow Characteristics

The pressure of the mercury vapor in the tube was considered a prime variable. The necessity of maintaining elevated tube temperatures made pressure measurements in the micron range by conventional means extremely difficult. A condensing temperature technique was tried, but the thermal lag and difficulty of observing the onset of condensation rendered the method useless except as a rough estimate. The normal environmental pressure in which the thrusters operate is of the order of 10^{-5} torr, which is negligible compared with the pressure drop across the tube. The tube pressure drop (assuming it exhausts into a perfect vacuum), which is in the micron range, would thus be a good estimate of the mean absolute pressure in the tube.

The pressure drop across the isolation device (tube and grid) calculated by the method of reference 5 is shown in figure 6. The calculation was made for tube diameters of 2.5 and 5.1 centimeters and included the

pressure drop across the fine-mesh grids having surface areas of 44 and 84 square centimeters, respectively. The 5.1-centimeter-diameter tube was used throughout the investigation because of its low pressure drop characteristics. The fine-mesh grid with 84 square centimeters of surface area contributed a maximum pressure drop of about 2 microns at the maximum propellant flow rate of 1.25 amperes. This grid was used in most of the investigation although a coarse-mesh grid of still lower pressure drop was also investigated.

Low Propellant Current Density

Fine mesh grid. - The design-point neutral in-flow current density in a 5-centimeter-diameter thruster is of the order of 40 amperes per square meter (based on anode diameter) and is obtainable with a 0.127-centimeter-diameter orifice. At an equivalent neutral propellant flow rate of 0.078 ampere, the calculated tube pressure is about 2 microns. The performance of the isolation tube at various thruster filament-emission currents is shown as a function of net accelerating voltage in figure 7. The potential of the grid, which was in floating mode, was relatively independent of both filament-emission current and net accelerating voltage and remained at a value close to the ionization-chamber potential difference of 50 volts (fig. 7(b)). The critical voltage, at which a tube discharge occurred (shown as a solid symbol), was likewise relatively independent of emission current. These results were somewhat surprising since an increased emission current results in an increased plasma density that can be visually observed by the relative intensity of the blue glow (excitation) filling the containment grid. It was expected that a high plasma density at the grid would render the isolation tube more susceptible to a discharge, but the data in figure 7 show this is not the case.

The leakage to ground (fig. 7(a)) followed expected trends. The leakage currents indicated by solid symbols were obtained shortly before onset of the tube discharge, which was of the order of 1 or 2 amperes. The values are thus orders of magnitudes lower than the currents after discharge.

Results of isolation grid operation at -50 volts bias relative to the net accelerating, or anode, voltage are shown in figure 8. The critical voltages and the leakage currents (fig. 8(a)) were similar to those of the floating grid operation.

The grid was also operated in a positively biased mode and the results are shown in figure 9. With the grid biased at 5 volts, positive relative to the anode, the leakage current increased (fig. 9(a)) and the beam current was reduced. The tube under this positive bias condition contained a pale glow discharge that extended a short distance upstream from the containment grid toward the grounded vaporizer. Reducing the positive bias caused this glow to grow dimmer until at a negative bias voltage (with respect to the anode), the entire region between the vaporizer and the grid was again void of any visible discharge. The existence of a relatively

high leakage current in positive bias operation, however, did not adversely affect the critical voltage before onset of a tube discharge. Higher positive grid bias voltages caused a runaway condition in the leakage current that ultimately led to a breakdown discharge in the tube.

Coarse mesh grid. - A containment grid with a mean open dimension 3.5 times larger than the first grid (both grids shown in fig. 3) was operated in floating mode, and the results are shown in figure 10. Grid voltage (fig. 10(b)) and leakage current (fig. 10(a)) were similar to those obtained with the fine-mesh grid at comparable conditions. The critical net accelerating voltages were about 500 volts lower than those obtained with the fine mesh but were again substantially independent of the filament-emission-current level.

High Propellant Current Density

In order to raise the tube pressure and to substantiate further the flow-handling capability of the isolation system, a 20-centimeter-diameter thruster was operated at equivalent neutral propellant flow rates of 0.97 and 1.25 amperes. At these flow rates, the average neutral current density entering the thruster is about 30 amperes per square meter (based on anode diameter). The neutral current density in the 5.08-centimeter-diameter tube was 240 amperes per square meter, resulting in a calculated tube pressure of about 10 microns (fig. 6). This pressure is considered approximately correct as attested by the gradual accumulation of condensed mercury within the tube during sustained operation at tube temperatures of about 40° to 50° C.

The results of the runs at high propellant flow rates are shown in figures 11 and 12. Unfortunately, floating-grid potentials were not measured during these runs. Leakage currents were again in the range of 3 to 10 microamperes, and the grid potential was thus expected to be around 30 or 40 volts negative with respect to the anode.

The beam current obtained at various values of filament-emission current and net accelerating voltage is shown in figure 11 for a neutral propellant flow of 0.970 ampere. At a net accelerating voltage of 4500 volts, propellant-utilization efficiency of 70 percent was attained at an energy dissipation of 500 electron volts per ion. The critical voltage at two levels of filament-emission current was around 6000 to 6500 volts, not greatly different from the results obtained with the 5-centimeter-diameter thruster.

The data for leakage currents shown in figures 11 and 12 indicate that the increased plasma density caused by increased cathode emission current may be responsible for increases in leakage current. The results of operation at 1.25 amperes neutral propellant flow are shown in figure 12. The thruster encountered considerable operational difficulty at this flow rate. Accelerator impingement current was excessively high at lower net accelerating voltages, and frequent interelectrode breakdowns were encountered at

higher voltages and emission currents. The critical voltages for onset of tube discharge during reasonably stable thruster operation were again in the neighborhood of 5500 to 6000 volts.

Operation at Elevated Tube Pressure

As an indication of possible derating of the isolation device at high tube pressures, some results taken with a 5-centimeter-diameter thruster are shown in figure 13. These results are not conclusive because of the double-orifice technique used to obtain the elevated tube pressures. In addition, the beam-current neutral-propellant-flow characteristics of the thruster obtained in a previous investigation were used as an indication of actual neutral propellant flow rate. If it is assumed that the propellant flow rate is known, a secondary orifice of a proper size placed between the grid and the thruster allows the thruster to operate at normal neutral current density, while a range of calculable tube pressures can be obtained by using a primary orifice of various sizes. Under these conditions, however, the glow of the ionization chamber was visible on the grid only as a spot formed by the beam passing through the secondary orifice.

As might be expected, the critical voltage decreased with increasing tube pressure. Some indications also exist that the coarse-mesh grid may derate more rapidly at high pressures.

Also shown in figure 13 is the Paschen curve of sparking potential for air and other gases of similar molecular weights (ref. 3). The conventional parameter Pd (pressure times distance) was reduced to pressure alone on the bases of a 5.1-centimeter tube diameter and of a distance of 25.4 centimeters between the tip of the grid and the grounded vaporizer. Although mercury vapor was not one of the gases included in the curve of reference 3, the difference between the grid-contained critical voltages and the sparking potential of plane parallel electrodes in nonionized gases is considerable.

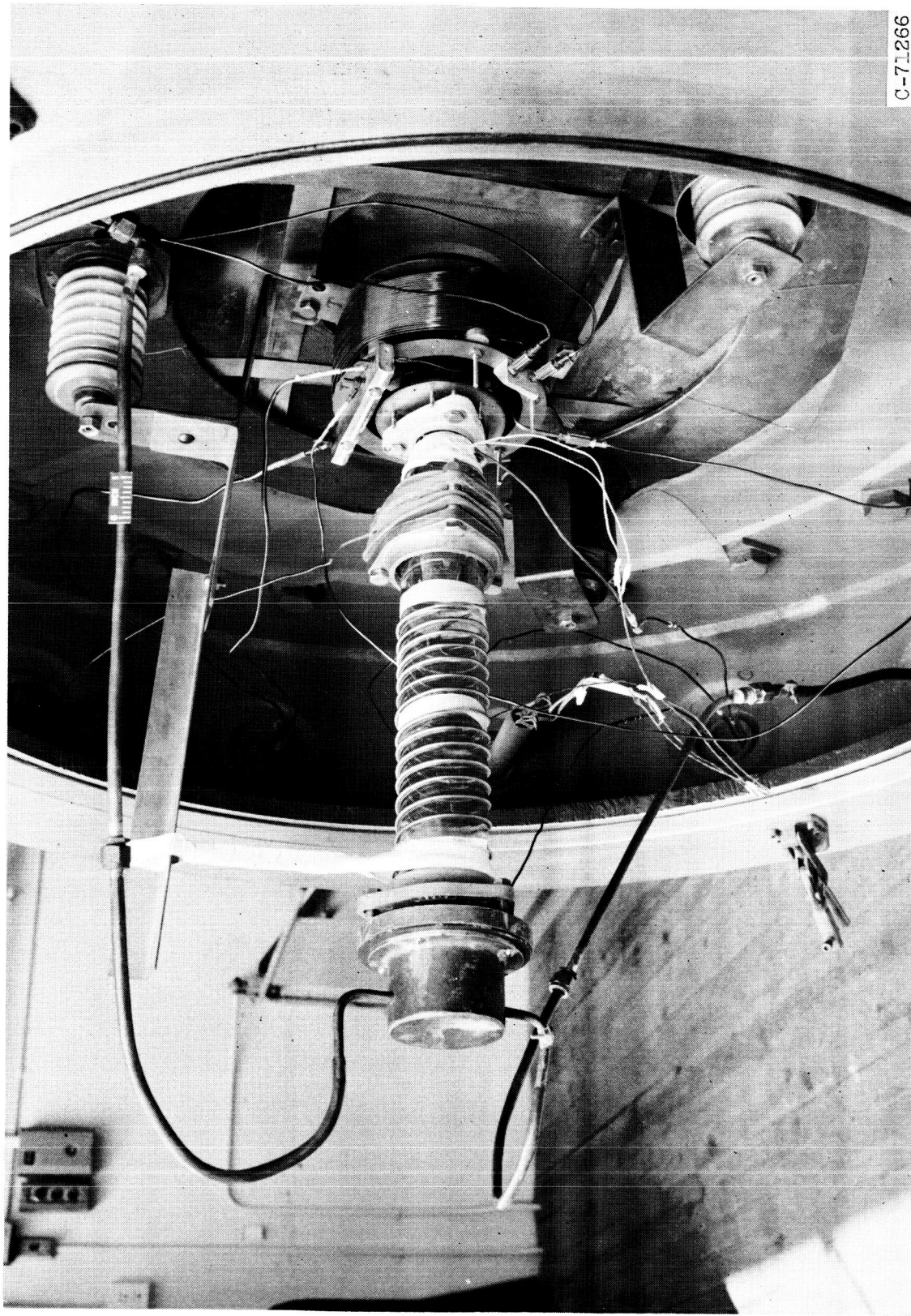
CONCLUDING REMARKS

Preliminary results indicate that a simple passive isolation device can maintain potentials as high as 5 to 6 kilovolts between an operating thruster and a grounded propellant-vapor source. Although the mechanism that triggers the tube discharge is not clearly understood, there are indications that the critical voltage may be determined by arcing discharges that occur within the thruster.

The preliminary information reported herein shows that a plasma containment grid in the propellant-feed tube is a promising solution to the thruster-propellant tankage-isolation problem. Further investigations should be conducted to evaluate this concept fully.

REFERENCES

1. Kaufman, Harold R.: An Ion Rocket with an Electron-Bombardment Ion Source. NASA TN D-585, 1961.
2. Mickelsen, William R., and Kaufman, Harold R.: Status of Electrostatic Thrusters for Space Propulsion. NASA TN D-2172, 1964.
3. Cobine, James D.: Gaseous Conductors: Theory and Engineering Applications. Dover Publications, Inc., New York, 1958.
4. Stover, John B.: Electric Breakdown and Arcing in Experimental Ion Thruster Systems. AIAA Paper 63057, 1963.
5. Dushman, Saul: Scientific Foundations of Vacuum Technique. John Wiley & Sons, Inc., New York, 1949.



C-71266

Figure 1. - Vacuum-facility installation of ion thruster with propellant vapor source and high-voltage isolation tube.

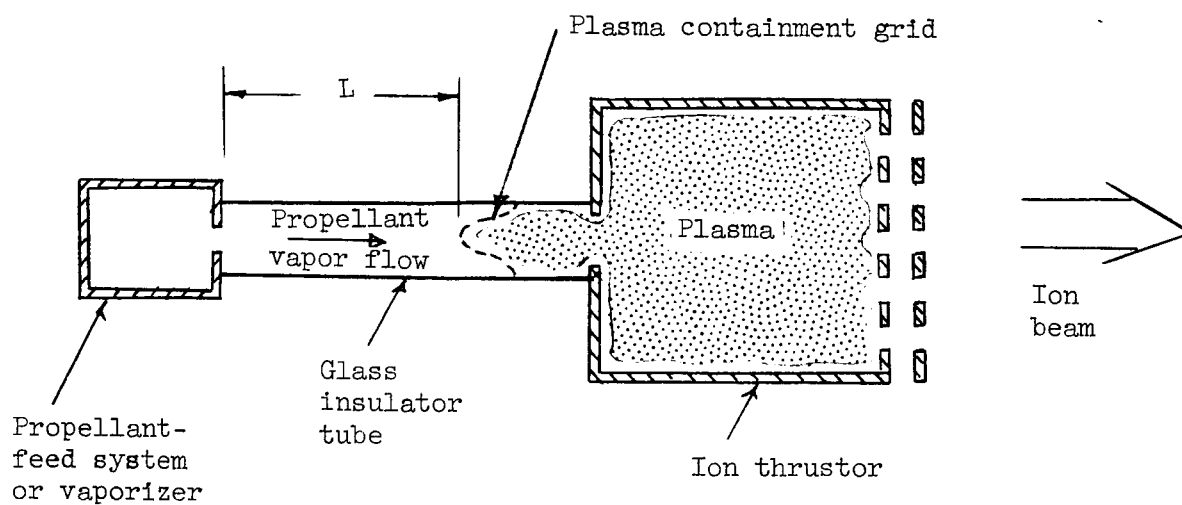
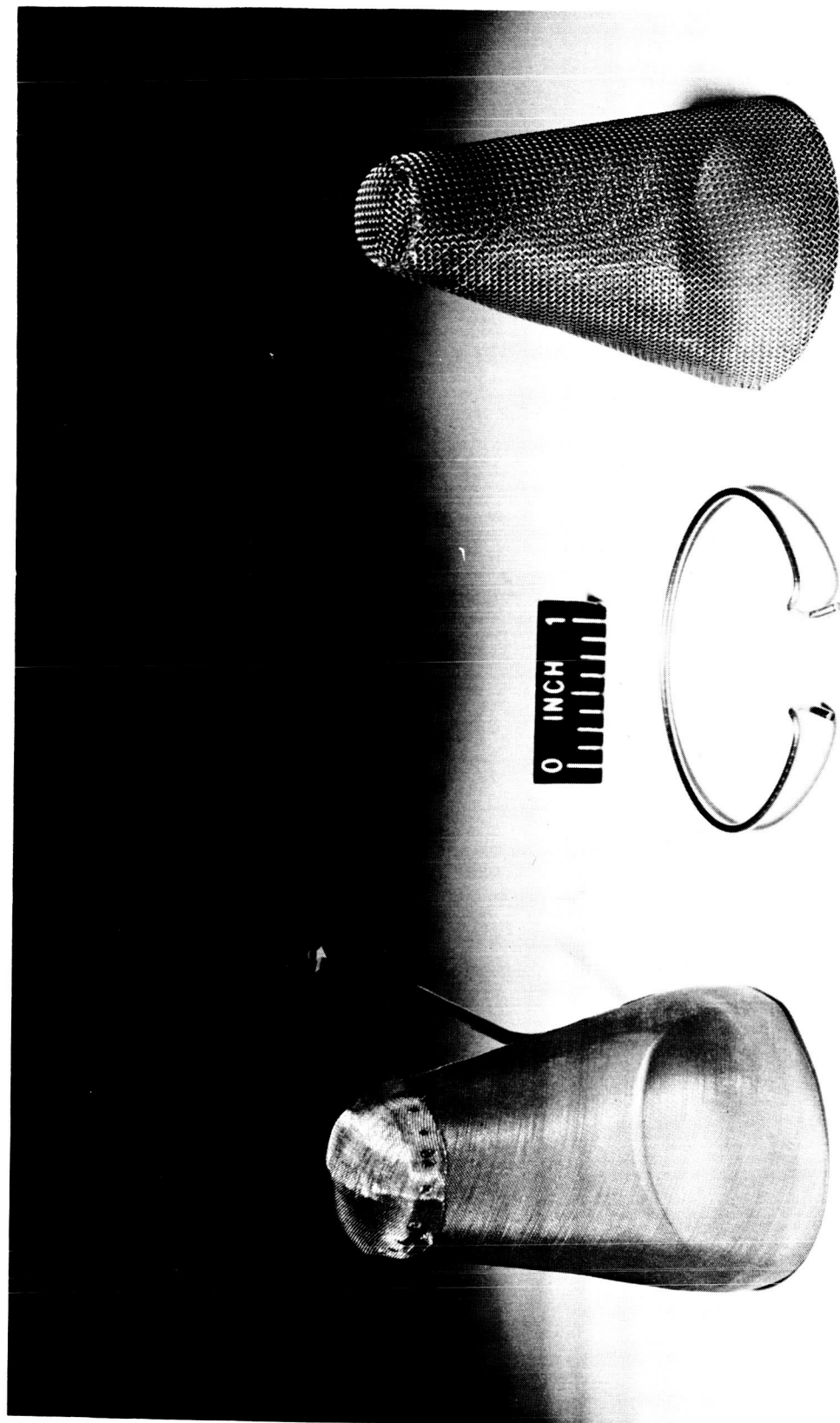


Figure 2. - Schematic drawing of propellant-feed isolation device.



C-71264

Figure 3. - Fine- and coarse-mesh grids with retaining ring.

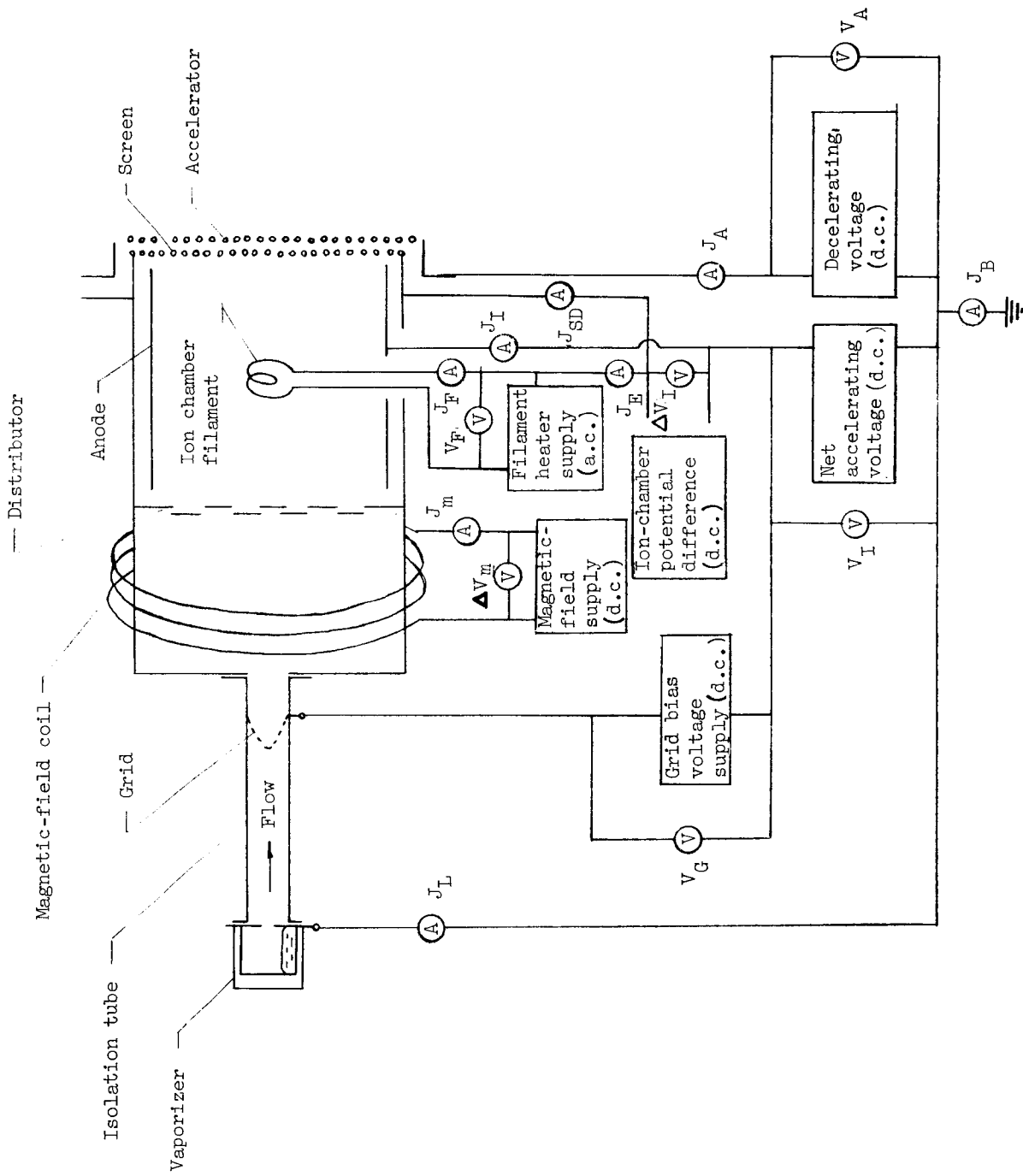
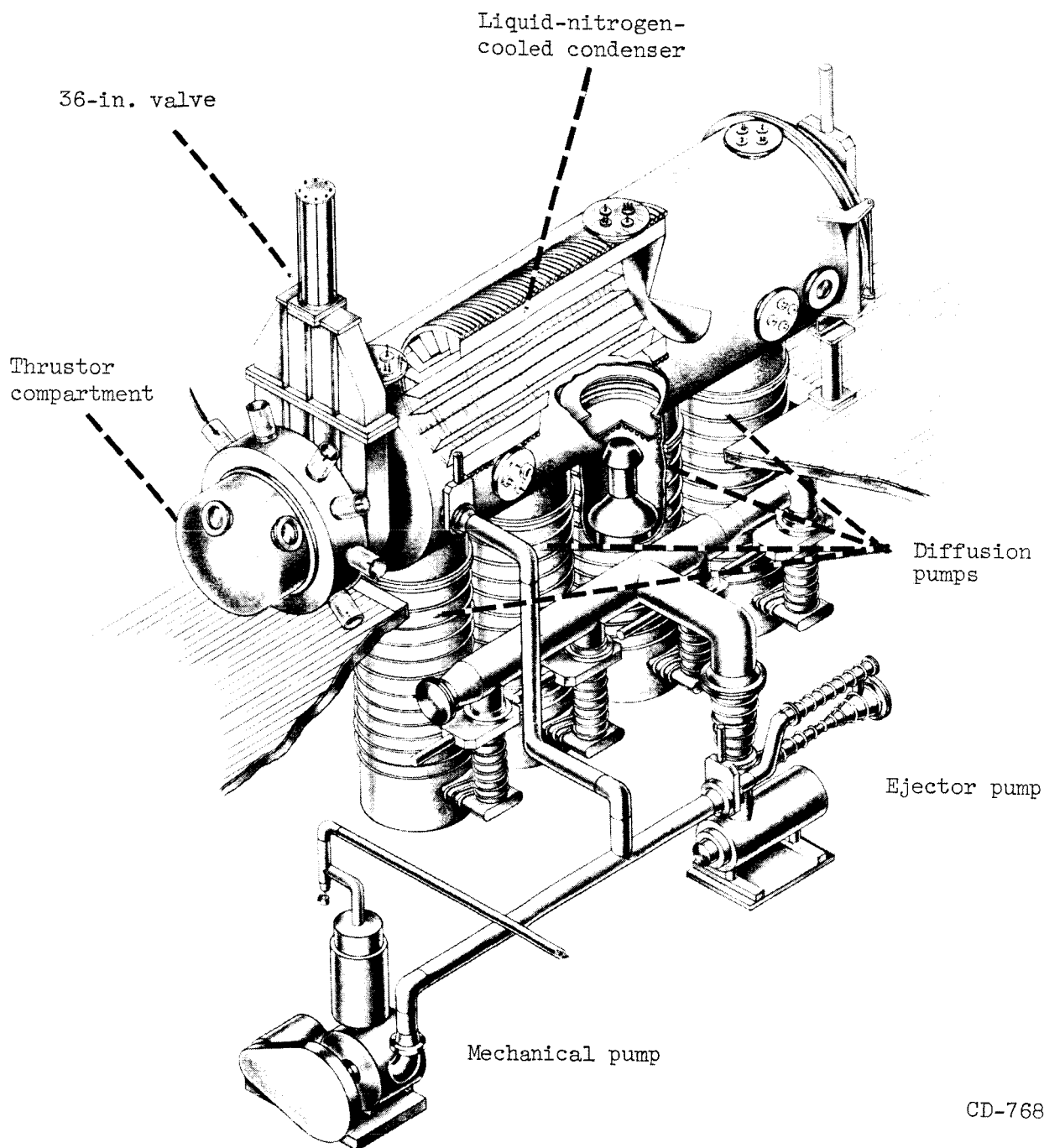


Figure 4. - Wiring diagram of ion thruster and propellant-feed isolation device.



CD-7687

Figure 5. - Vacuum facility.

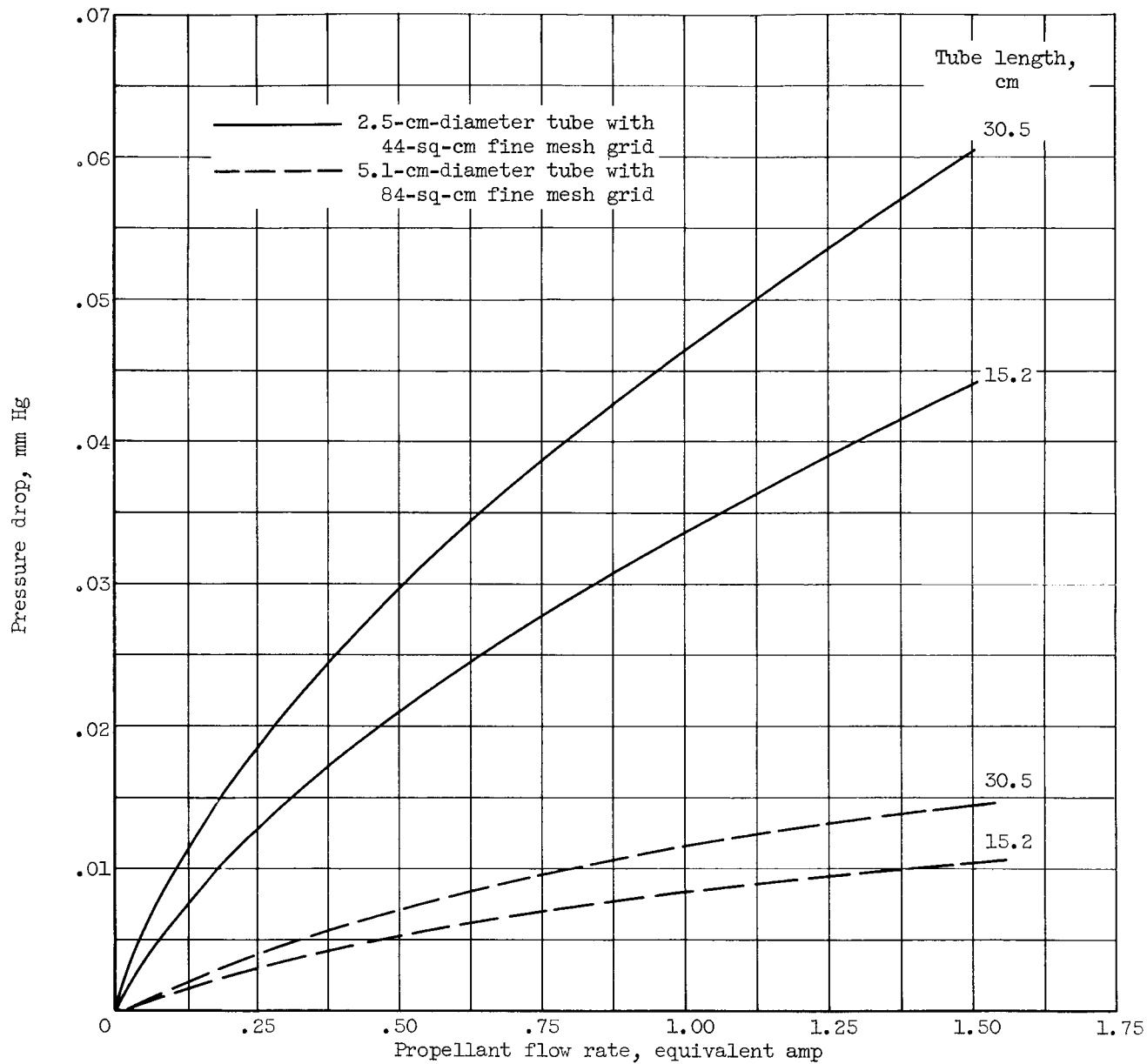
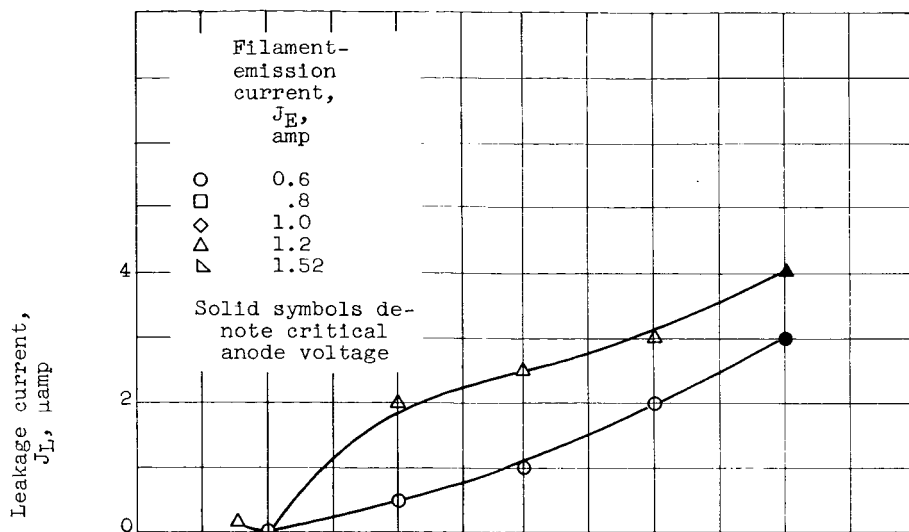
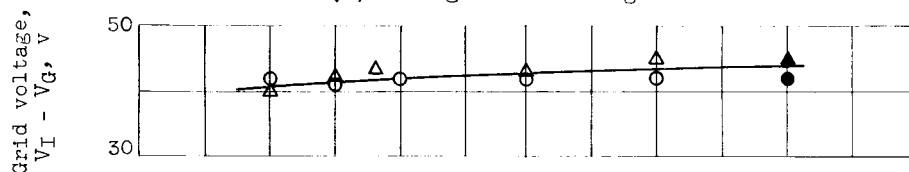


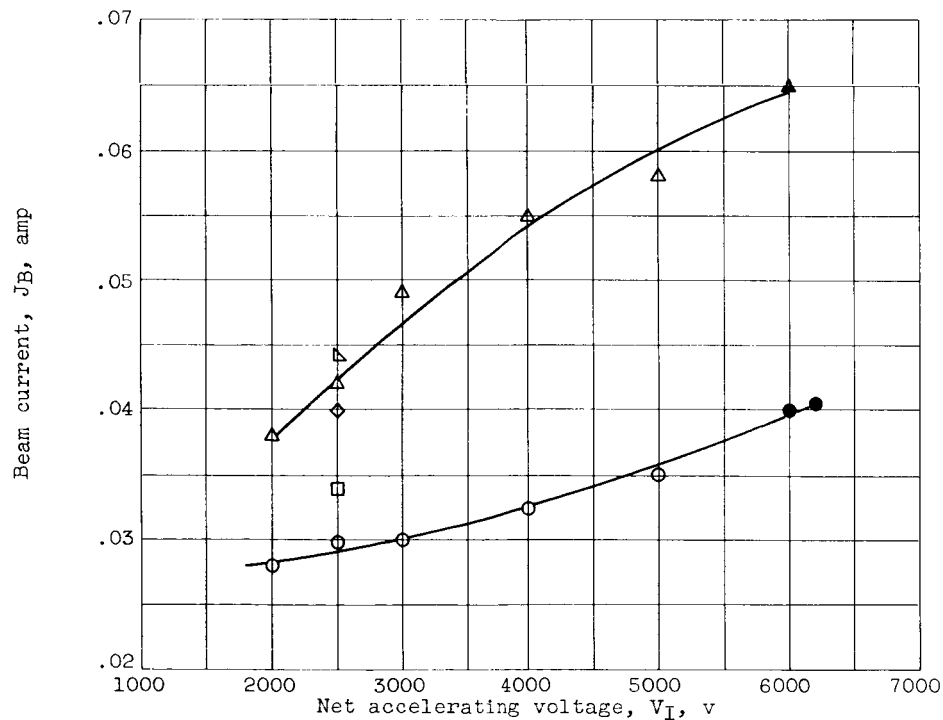
Figure 6. - Calculated pressure drop across isolation tubes and grids as function of propellant flow rate.



(a) Leakage current to ground.

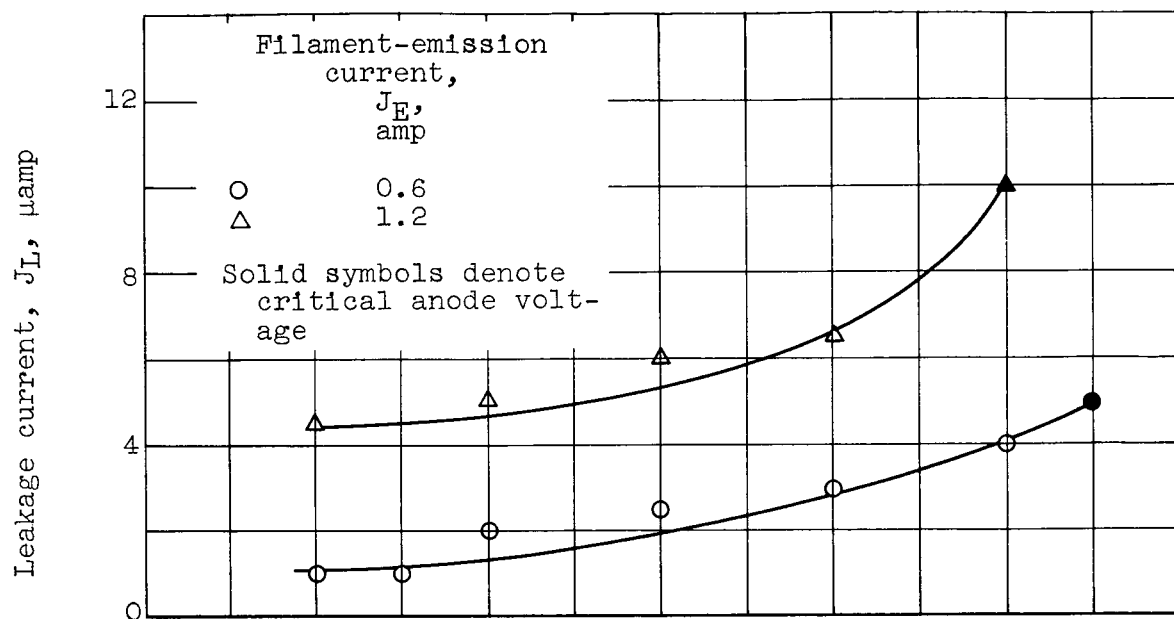


(b) Grid voltage to anode.

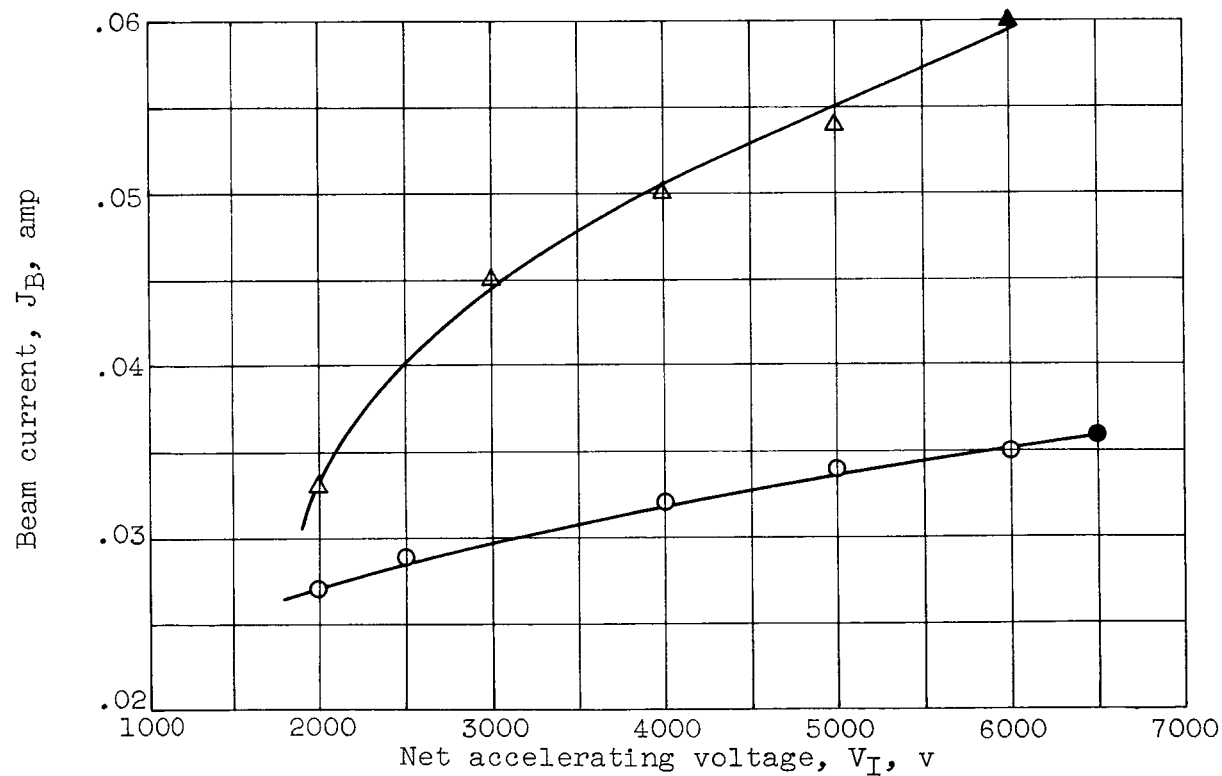


(c) Beam current.

Figure 7. - Performance characteristics of isolation device with fine-mesh grid at floating potential. Propellant flow rate equivalent, 0.078 ampere; thruster diameter, 5 centimeters.

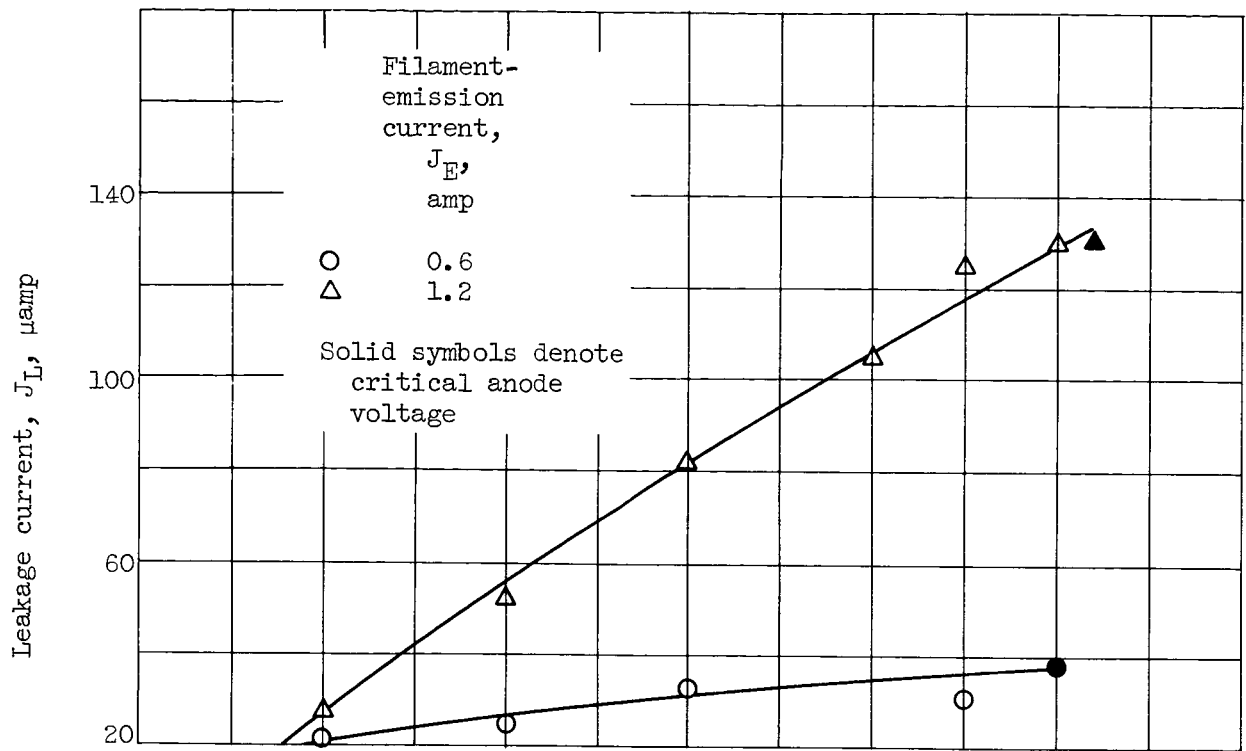


(a) Leakage current to ground.

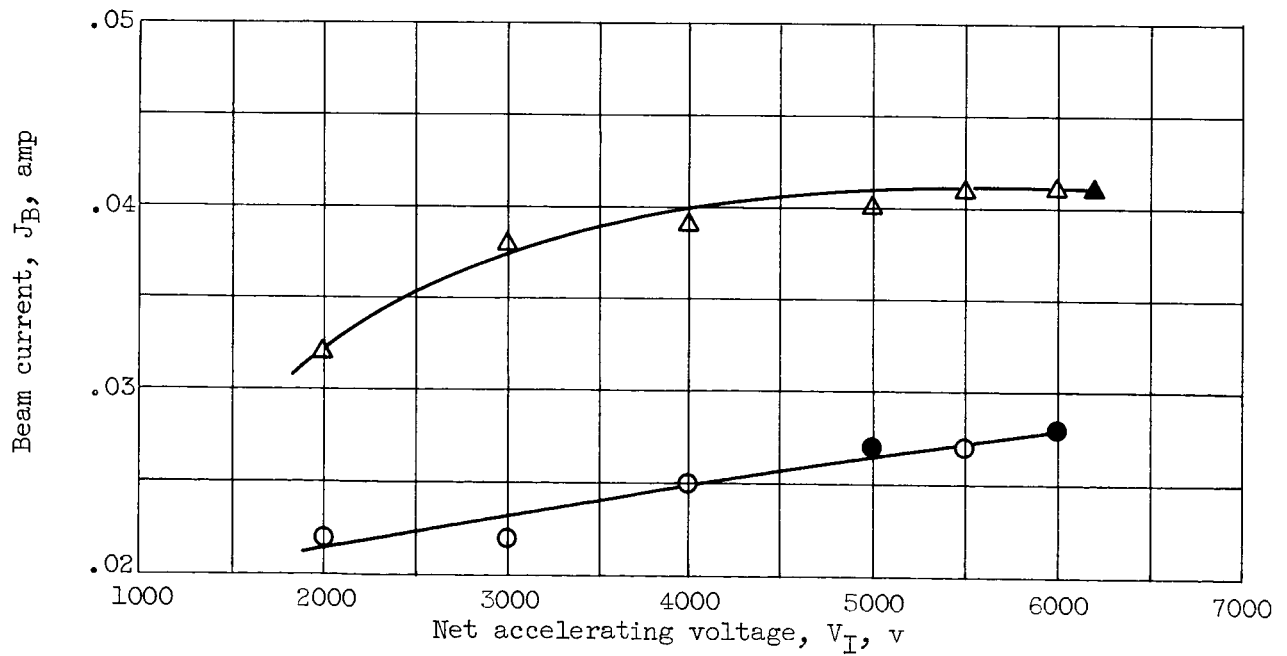


(b) Beam current.

Figure 8. - Performance characteristics of isolation device with fine-mesh grid biased at -50 volts. Propellant flow rate equivalent, 0.078 ampere; thruster diameter, 5 centimeters.

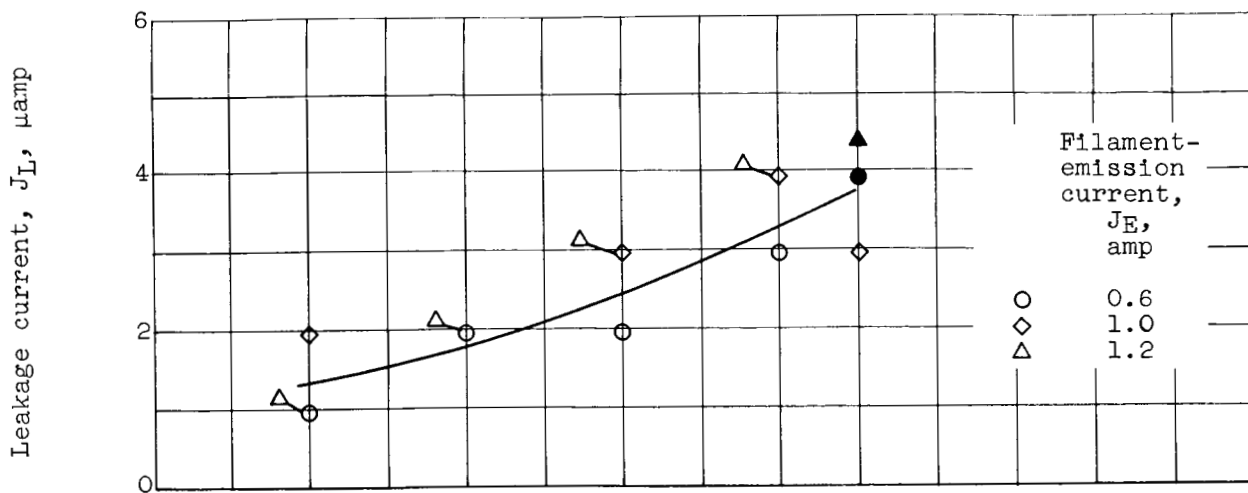


(a) Leakage current to ground.

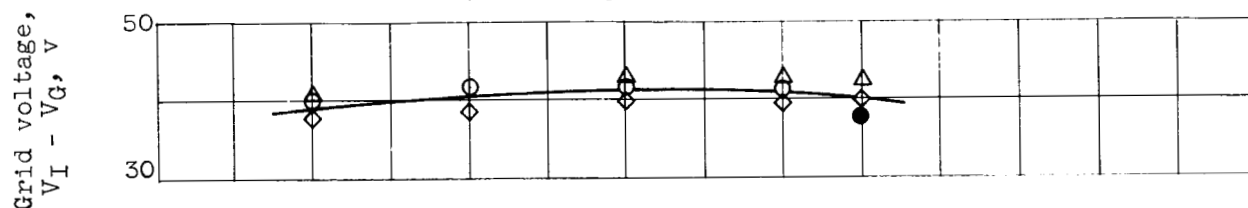


(b) Beam current.

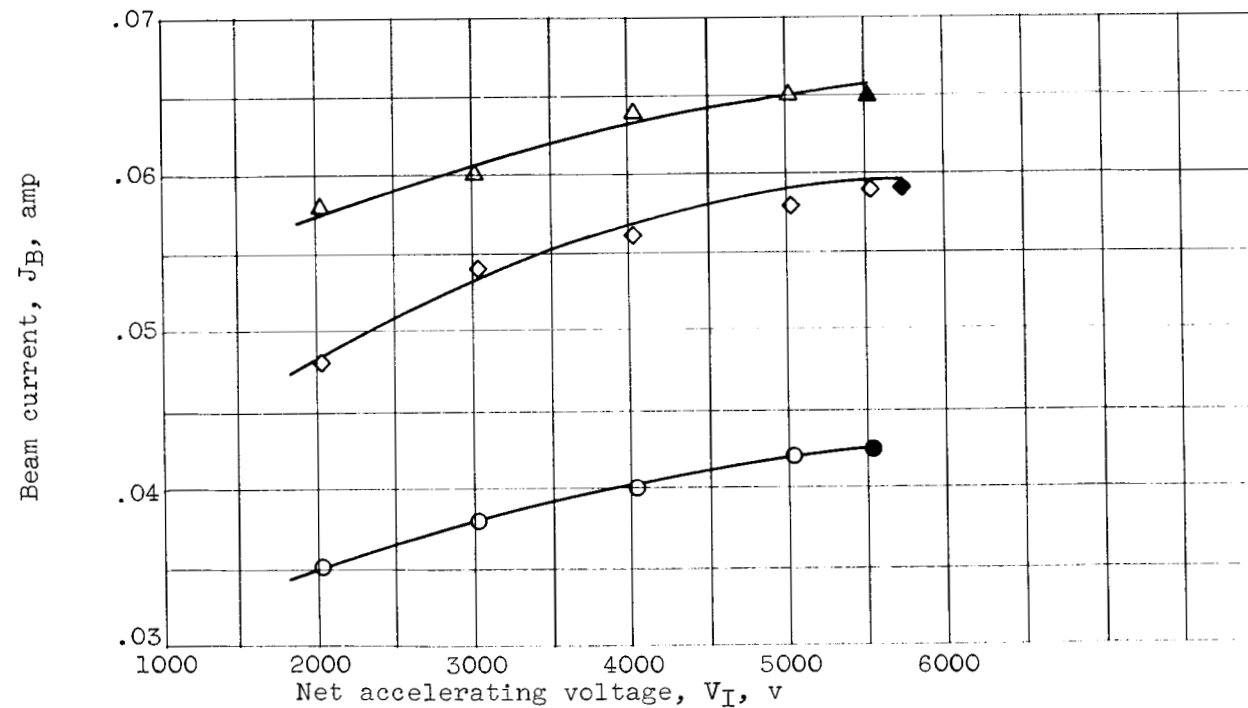
Figure 9. - Performance characteristics of isolation device with fine-mesh grid biased at 5 volts. Propellant flow rate equivalent, 0.078 ampere; thruster diameter, 5 centimeters.



(a) Leakage current to ground.

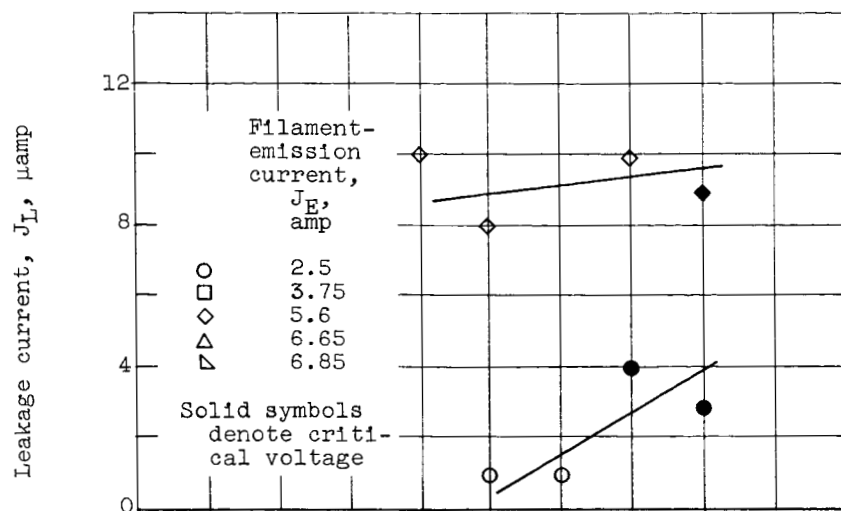


(b) Grid voltage relative to anode.

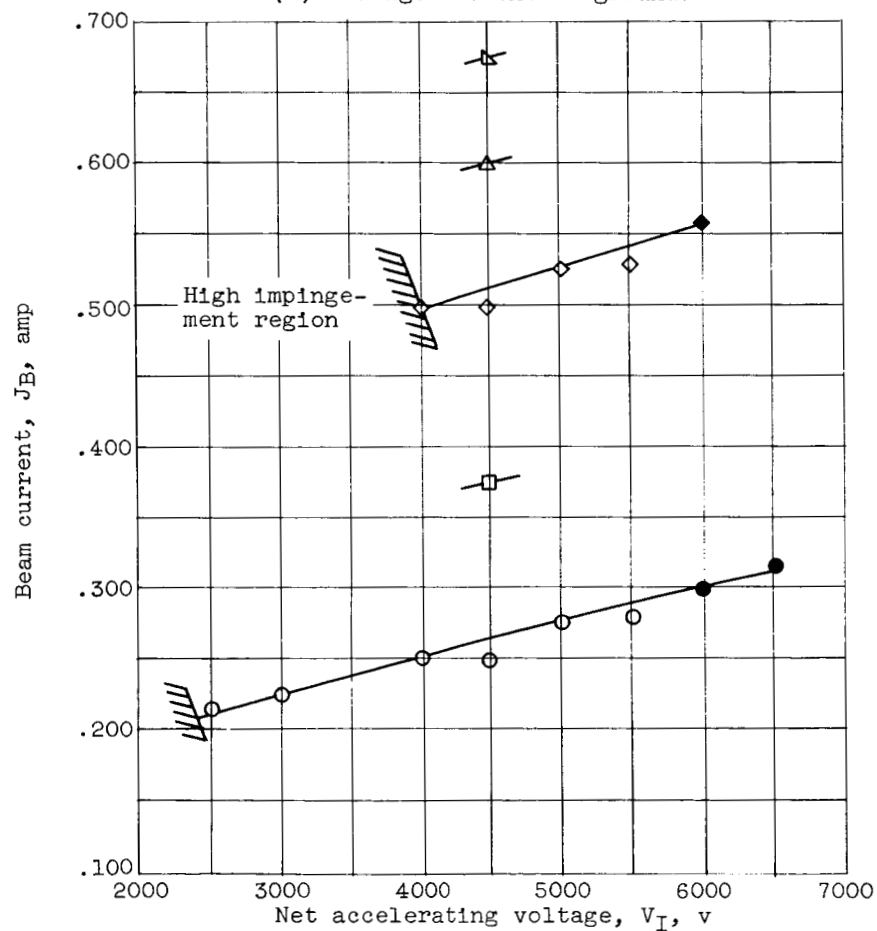


(c) Beam current.

Figure 10. - Performance characteristics of isolation device with coarse-mesh grid at floating potential. Propellant flow rate equivalent, 0.078 ampere; thruster diameter, 5 centimeters.

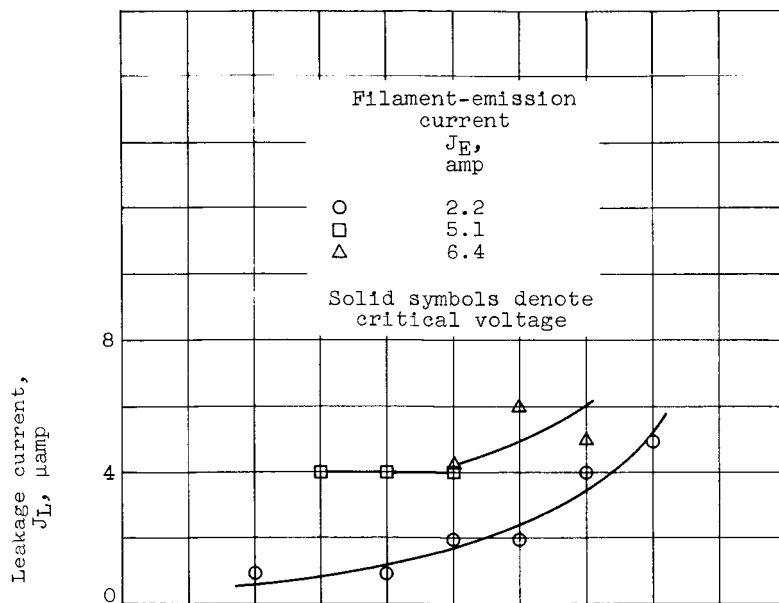


(a) Leakage current to ground.

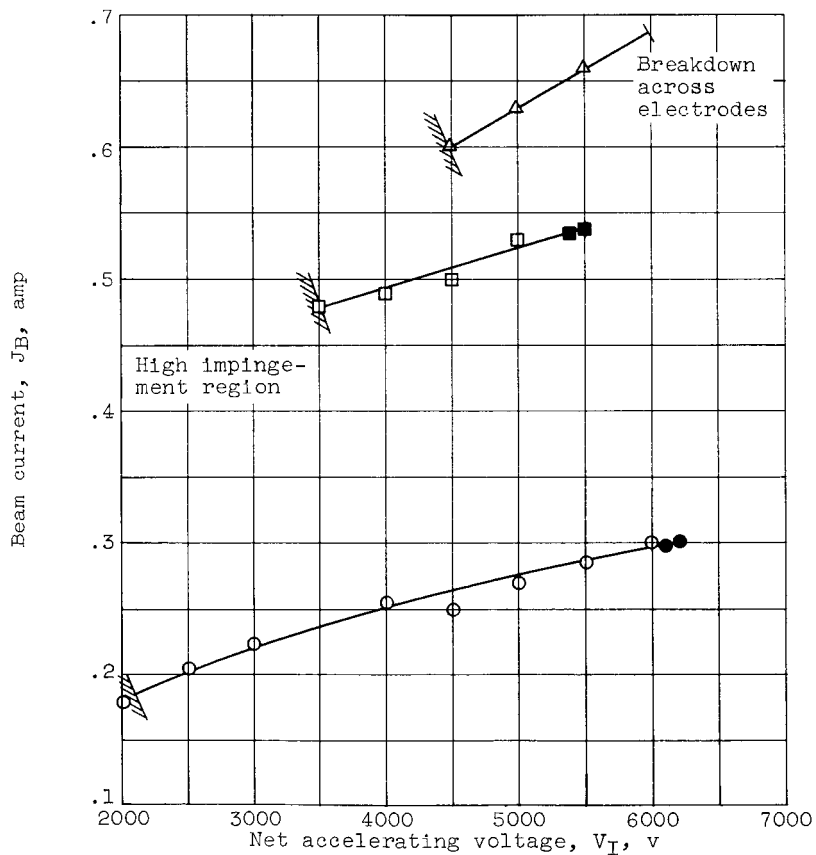


(b) Beam current.

Figure 11. - Performance characteristics of isolation device with fine-mesh grid at floating potential. Propellant flow rate equivalent, 0.97 ampere; thruster diameter, 20 centimeters.



(a) Leakage current to ground.



(b) Beam current.

Figure 12. - Performance characteristics of isolation device with fine-mesh grid at floating potential. Propellant flow rate equivalent, 1.25 amperes; thruster diameter, 20 centimeters.

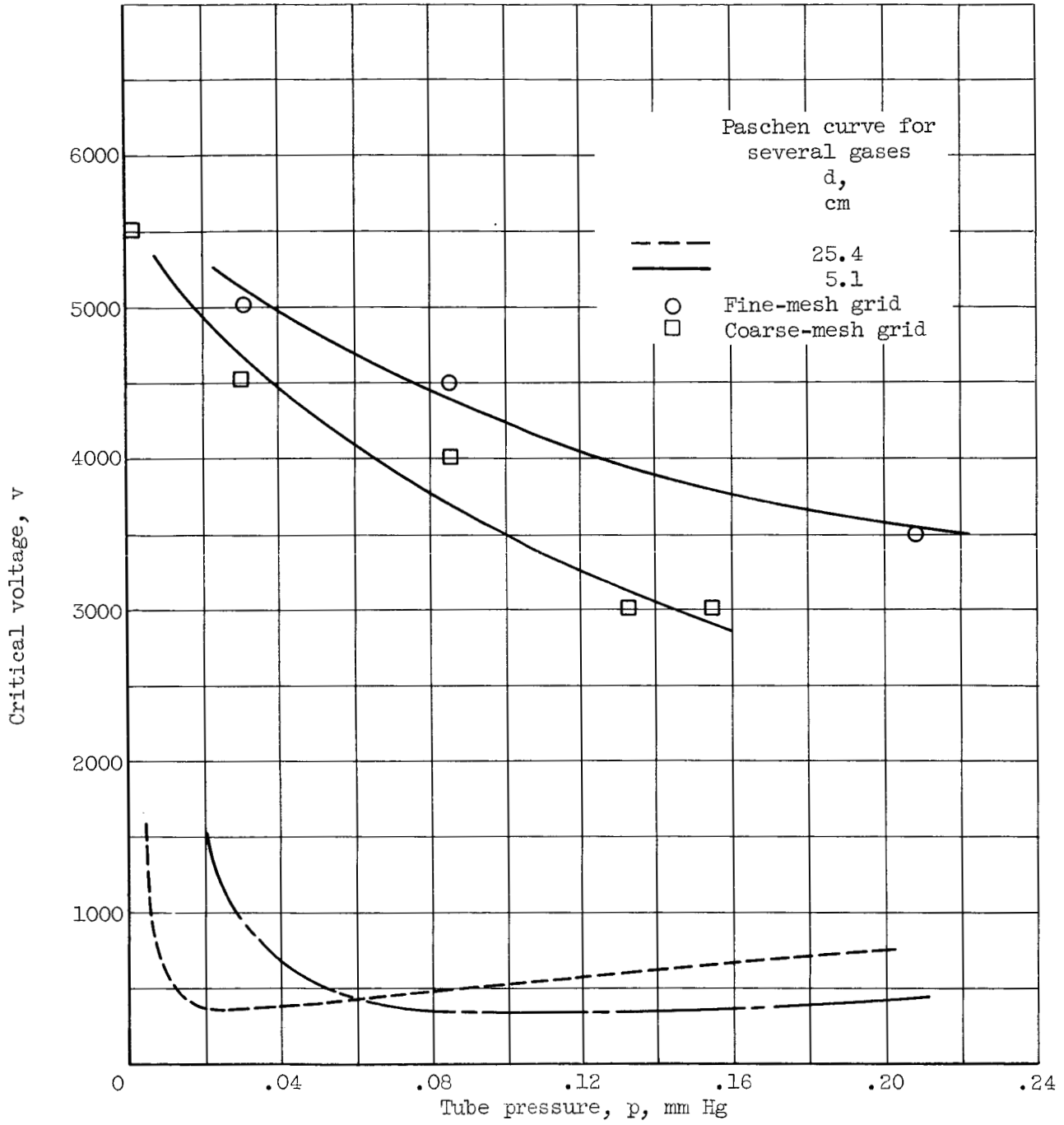


Figure 13. - Critical voltage as function of gas pressure. Isolation-tube diameter, 5.1 centimeters; effective length, 25.4 centimeters.